Green Chemistry

PAPER

View Article Online
View Journal | View Issue

Cite this: *Green Chem.*, 2018, **20**, 3566

Elucidating transfer hydrogenation mechanisms in non-catalytic lignin depolymerization†

Florent P. Bouxin,[a] Henri Strub,[b] Tanmoy Dutta,[a,c] Julie Aguilhon,[b] Trevor J. Morgan,[d] Florence Mingardon,[e] Murthy Konda,[a] Seema Singh,[a,c] Blake Simmons[a] and Anthe George *[a,c]

Lignin undergoes catalytic depolymerization in the presence of a variety of transfer hydrogenation agents, however the mechanisms for non-catalytic depolymerization of lignin *via* transfer hydrogenation are not well understood; this makes process optimization difficult. Herein, for the first time a mechanism for this process is proposed. For the purposes of understanding the mechanisms involved in these non-catalytic lignin depolymerization processes, this study investigates the equilibrium system of formic acid, methyl formate and carbon monoxide, as agents for the depolymerization of lignin, in the presence of either water or methanol as solvents. In the methyl formate/water (at 300 °C) system, 73 wt% oil was produced which contained a significant amount of low molecular weight alkylphenols, with less than 1 wt% char produced. In aqueous media, the results showed that methyl formate maintains an equilibrium with formic acid which is itself in equilibrium with carbon monoxide. It was found that using either formic acid or methyl formate for non-catalytic transfer hydrogenation of lignin can produce high amounts of oil, and can be described as a two-stage mechanism. After 10 min of reaction at 300 °C, around a quarter of the formic acid is consumed *via* hydride transfer of the formate proton, preventing the condensation of lignin fragments. At the same time, approximately three quarters of the formic acid decomposes to carbon dioxide and carbon monoxide. Once the formic acid is consumed, the carbon monoxide was identified as the precursor to a reactive reductive reagent and was able to activate the proton of the water molecule preventing further condensation of the lignin fragments. It has been previously thought that transfer hydrogenation in lignin using formic acid occurs *via* the production of molecular hydrogen. Here it is demonstrated that formic acid reacts directly with the lignin, without this hydrogen formation. Therefore the key parameters for efficient transfer hydrogenation of the lignin to maximize bio-oil yield appear to involve controlling the reactions between lignin and formic acid, methyl formate or carbon monoxide under aqueous conditions, thereby reducing the reagent cost and loading while maintaining efficient lignin conversion.

Received 27th October 2017,
Accepted 23rd March 2018

DOI: 10.1039/c7gc03239k

rsc.li/greenchem

Introduction

The environmental impact of fossil fuel consumption is increasing and the transition to more sustainable energy is underway. More environmentally benign methods for producing energy are developing and biomass has a key role to play in these mitigation strategies. For the past decade, significant efforts have been made in the production of lignocellulosic biofuels.[1] Several biofuel processes based on biological conversion of the cellulosic fraction of the pretreated biomass are at the scale-up phase. However, the economic viability of such processes requires the valorization of the lignin fraction.[2] Currently, lignin is usually burned for process heat. However, lignin could be more profitable as a feedstock for the production of bulk aromatic bio-based synthons.[3]

The depolymerization of lignin to lower molecular weight is often seen as the critical step for its efficient valorization.[4] Improving our understanding of the lignin depolymerization and charring mechanisms has significance in a number of related areas of study such as the production of alternative and biomass derived biofuels. For example, there is a need for a pathway to produce low molecular weight aromatics as addi-

[a]*Joint BioEnergy Institute, Lawrence Berkeley National Laboratory, Berkeley, CA 94720, USA. E-mail: ageorge@lbl.gov*
[b]*Total Raffinage Chimie, 2 Pl. Jean Millier, 92400 Courbevoie, France*
[c]*Biological and Engineering Sciences Center, Sandia National Laboratories, Livermore, California 94551, USA*
[d]*Hawaii Natural Energy Institute, University of Hawaii at Manoa, Honolulu, Hawaii, 96822, USA*
[e]*Total New Energies Inc., Emeryville, CA, USA*

†Electronic supplementary information (ESI) available. See DOI: 10.1039/c7gc03239k

tives to aliphatic oils produced *via* the hydrotreated esters and fatty acids (HEFA) process.[5–8] Understanding biomass and more specifically lignin reaction mechanisms is also vital for the optimization of bio-carbon production through methods such as hydrothermal carbonization, flash carbonization™ and constant volume pyrolysis.[9–11] All these areas of study rely on the control, and thereby understanding, of reaction conditions to tailor product properties while reducing costs.

Reductive approaches for the depolymerization of lignin have recently received significant attention.[4,12,13] Among them, catalytic depolymerization of lignin in the presence of hydrogen has been extensively studied.[13–15] It is well established that formic acid (FA) can be used as an *in situ* source of hydrogen and is often used in combination with noble metal catalysts for the depolymerization and deoxygenation of the lignin (Table S.1†). Previous studies reported the efficient depolymerization of lignin in FA-water media using bifunctional noble metal catalysts or in isopropanol-FA media using Ru/C catalyst.[16,17] In these two studies, the non-catalytic control conditions were reported to generate significantly lower amounts of oil and higher amount of char. On the other hand, the addition of a noble metal catalyst limited char production and increased the monomeric phenolic yields. Inversely, another study at lower temperatures (265 °C) showed that the oil yield was not improved when the Pd/C catalyst was added in the system. In non-catalytic and catalytic conditions, catechol (1,2-dihydroxybenzene, CAS 120-80-9) was the major product of the monomeric fraction.[12] In alkaline conditions, another study reported that the depolymerization of eucalyptus lignin in the presence of sodium formate at 300 °C in water led to guaiacol (2-methoxyphenol, CAS 90-05-1) and syringol (1,3-dimethoxy-2-hydroxybenzene, CAS 91-10-1) as the main products.[18] In a recent study, Onwudili *et al.* used a two-stage catalytic hydrothermal process to depolymerize lignin to phenols. Interestingly, the author reported higher oil yield as well as monomer yield using non-catalytic conditions. On the other hand, a greater amount of char was produced in catalytic conditions which could be attributed to the use of an acidic alumina supported Pt catalyst which is known to favor coking.[19] According to previous studies, the non-catalytic transfer hydrogenation of lignin produced similar or higher yields of oils. Moreover, the use of noble metal catalysts are expensive and their recycle challenging. In that context, optimizing lignin depolymerization in non-catalytic conditions using transfer hydrogenation type reactions is a desirable approach. A recent study showed promising results for the lignin conversion to bio-oil using FA in non-catalytic aqueous media. The authors achieved up to 75% oil yield for the softwood Kraft lignin conversion at 390 °C and 4 h reaction. The authors highlighted the slight increase of oil yield in ethanol-based conditions and attributed this to the alkylation of the lignin fragments.[20]

In other work, non-catalytic transfer hydrogenation using FA in alcohol media was applied to a series of lignin model compounds in order to understand the degradation or depolymerization mechanisms. At temperatures around 350 °C, the authors concluded that the mechanism propagates through the homolytic cleavage of the ether bonds. Moreover, the authors made the assumption that the molecular hydrogen, produced from the FA decomposition, suppressed recondensation of the lignin fragment.[21] A recent study on hardwood lignin depolymerization in subcritical water under different gases (N_2, CO, H_2 and CO_2) reported similar lignin conversion regardless of the gases used. However, the authors reported that carbon monoxide generated the best environment for the production of low molecular weight products.[22] Other studies reported the effect of carbon monoxide and water in the depolymerization of lignin. In the presence of sodium carbonate, up to 90% of the lignin products were benzene soluble after reaction at 380 °C and 1500 psi of carbon monoxide (cold pressure). The authors also suggested that the carbon monoxide was able to cleave β-ether linkages of the lignin.[23]

Under subcritical water conditions, decarboxylation of FA was observed and carbon monoxide production from the lignin decomposition has been suggested.[12] However, at the same temperature other studies report that the FA decomposes *via* two pathways.[21] According to previous work, the decarbonylation and decarboxylation can be tuned depending on the temperature and acidity of the media. Under acidic conditions, decarbonylation will be preferred while basic conditions favour decarboxylation.[24] In other work, the decomposition pathway of the FA suggested that the isomer stability was the key to the FA decomposition route. In the presence of water, the *cis*-configuration gave the higher stability which suggested decarboxylation as the preferential pathway.[25] In an alcohol medium, FA was rapidly esterified due to the favorable equilibrium for alkylformate.[26] In previous work, an alcoholic media has been generally used. However, the quick esterification of the FA in the presence of the alcohol should have an impact on the activity of the formate as an H transfer donor reagent. The presence of water also had an impact on the reactivity of the FA. In that context, alkylformate could be substituted for FA in the water media.

Transfer hydrogenation of lignin in non-catalytic systems is likely to be a more attractive approach from an economic and process intensification perspective; a full techno-economic analysis would be required to assess such benefits and was not the focus of this study. However, there is a lack of understanding of the lignin transfer hydrogenation mechanisms, making process optimization challenging. In most of the previous studies, temperatures above 350 °C and reaction times as long as 15 h were required to produce high yields of low molecular weight phenolic compounds. The lignin loading was also kept below 10% and the mass ratio between FA and lignin was more than 2.[27,28]

In this study, non-catalytic transfer hydrogenation of sugarcane bagasse derived lignin was investigated. The study was designed to understand the key parameters permitting the minimization of lignin condensation reactions that produce char and the concomitant improvement in the production of deoxygenated lignin oils. The equilibrium system of FA, methyl formate (MF) and carbon monoxide was investigated.

First, aqueous and non-aqueous media were investigated *via* a parametric study of water or methanol as solvent, and FA or MF as reagent. The equilibrium was further investigated by evaluating the contribution of the system decomposition products, CO and H_2. A time-course study of the lignin depolymerization was then performed to observe the evolution of the product quantities and distributions. In parallel, the gas composition was measured as a function of the experimental conditions and reaction time in order to identify key conditions for efficient depolymerization of the lignin and minimization of char. Finally, deuterated FA was used to confirm the role of the hydride proton of the formate on the lignin deoxygenation process. From these studies, key mechanisms and reactions in the non-catalytic transfer hydrogenation of lignin were determined.

Results and discussion

Preparation of the bagasse lignin

The bagasse lignin was prepared from the saccharification residue of dilute acid pretreated sugarcane bagasse. The alkaline extraction permitted 73 wt% of the lignin initially present in the residue to be isolated. After alkaline extraction followed with acid precipitation, no sugars were detected in the isolated lignin which were composed of 88 wt% acid insoluble lignin (Klason Lignin) and 0.9 wt% ash. As illustrated in Table 1, significant amounts of nitrogen were observed which can be suggested to be from proteins bound to the lignin after precipitation. The molecular weight profile of the lignin showed a high polydispersity of 4.4 due to the presence of monomers *p*-coumaric acid and ferulic acid estimated to be 9.1 and 7.9 per 100 C_9 units of lignin. The presence of *p*-coumaric acid and ferulic acid in grass lignin was expected.[29] As illustrated in Table 1, the bagasse lignin is a syringyl rich lignin with 57% of syringyl (S) units, 34% of guaiacyl (G) and 8% of hydroxyphenyl (H) units. However, the *p*-coumaric acid and ferulic acid were not included in the lignin unit ratio as they are not considered to be part of the backbone of lignin; ferulic acid acts as bridge between lignin and hemicellulose components; coumaric acid is present as a pendent ester group on the lignin. Overestimation of both units in the lignin using 2D NMR has been reported. The abundance of alkyl aryl ether linkage (β-*O*-4) is 27% suggesting that the uncondensed structure was not significantly affected by the alkaline extraction. It is believed that the preservation of the uncondensed structure of the lignin is imperative to achieving good conversion into low molecular weight products.

Table 1 Characteristics of the bagasse sugar cane lignin [%S: syringyl units, %G: % guaiacyl units, %H: % *p*-hydroxyphenyl units; *p*CA: *p*-coumaric acid, FA: ferulic acid]

Elemental analysis				GPC analysis		
C	H	N	O	M_n	M_w	M_w/M_n
59.2	5.8	2.6	32.4	737	3214	4.4

NMR analysis							
%S	%G	%H	%pCA	%FA	% β-O-4	%β-5	%β–β
57.4	34.2	8.4	9.1	7.9	27.4	1.0	1.8

Parametric study of lignin transfer hydrogenation

Lignin depolymerization yields. In the first part of the study, the bagasse lignin underwent reaction in the presence of FA or MF with either methanol or water as the carrier solvent, to yield three products: (1) depolymerized lignin as an oil, (2) condensation products that formed char, and (3) degradation products that formed permanent gases. After reaction, the char was quantified as the insoluble fraction recovered after washing with a mixed solvent of tetrahydrofuran/methanol (2/1: v/v). The oil fraction was recovered after removal of the solvent. The unrecovered fraction corresponded to the complement of 100 wt% of the initial lignin. As illustrated in Fig. 1, 68 wt% to 73 wt% of the initial lignin weight was converted to oil after reaction. In the aqueous system, less than 2 wt% of the lignin was converted to char and from 27 wt% to 30 wt% of the initial mass of lignin was considered unrecovered (gas, water, methanol and some volatiles). In the MF/methanol system, the absence of water led to the production of 30 wt% char while the unrecovered fraction was similar to the FA/water condition (20–21%). The unrecovered fraction was up to 10% lower in the methanol system compared to the aqueous system. In the case of the FA/methanol system, the lower amount of unrecovered material was counteracted by the slightly higher production of char, around 6%. As a consequence, the aqueous system is more appropriate for the production of high amounts of oil while limiting char formation. Under aqueous conditions, the use of MF instead of FA had less effect on the yield of each product fraction compared to the methanol scenario. This could be explained by the fast hydrolysis of the MF to FA under aqueous reaction conditions.

Deoxygenation of lignin oil and char. As illustrated in Table 2, the elemental analysis of the oil and the char both

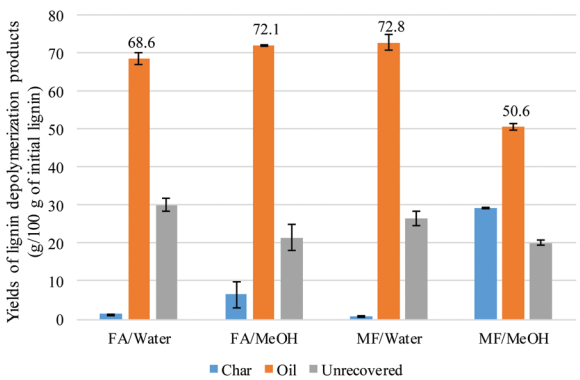

Fig. 1 % yields of the lignin depolymerization products (g per 100 g of the initial lignin) as function of the experimental conditions; values are the average of duplicate experiments.

Table 2 Elemental analysis of the oil and the char as a function of experimental conditions

	Oil g per 100 g of oil				Char g per 100 g of char				Oil + char (g per 100 g of bagasse lignin)			
	C	H	N	O	C	H	N	O	C	H	N	O
Bagasse lig.									59.2 (0.1)	5.8	2.6	32.4
FA/water	71.2	8.0	2.7	18.2	70.9	6.1	2.3	20.7	49.7 (0.8)	5.5	1.9	12.7
FA/MeOH	74.0	8.0	1.6	16.5	79.9	5.6	1.8	12.7	58.4 (0.8)	6.1	1.3	12.7
MF/water	70.1	8.2	1.8	20.0	72.7	6.3	1.7	19.3	51.4 (0.5)	6.0	1.3	14.7
MF/MeOH	73.1	7.8	2.1	17.0	81.6	5.6	2.4	10.4	60.9 (0.2)	5.6	1.8	11.6

showed reduced oxygen content compared to the initial bagasse lignin. The methanol system led to slightly higher deoxygenation of the oil with 16.5% and 17% of oxygen content in FA/methanol and MF/methanol condition respectively. More significant are the different oxygen contents in the chars. The absence of water generated a char with oxygen content as low as 10.4 wt% suggesting that the condensation led to the deoxygenation of the lignin. In other words, the methanol system favoured lignin condensation, increasing the deoxygenation of the oil but also produced more char that contained less oxygen. When the elemental compositions of the oil and char are added together, the deoxygenation was the least efficient under MF/water conditions and most effective under MF/methanol conditions. After taking into account the respective yield of oil and char, the combined elemental analysis of the oil and char was compared to the initial bagasse lignin elemental analysis. In that case, it is possible to follow the total amount of carbon recovered after transfer hydrogenation. As illustrated in Table 2, the carbon conservation was higher when methanol was used as solvent with 60.9 ± 0.2 wt% carbon conversion of the bagasse lignin which is slightly higher than the starting amount of carbon of 59.2 ± 0.1 wt%. This suggests that carbon was added to the lignin probably due to the methylation of the products.

Molecular weight distribution of the oil fractions. As illustrated in Fig. 2, all four conditions produced oils with lower M_w than the initial bagasse lignin. The MF/water system gave the oil with the lowest polydispersity with 1.93 and the lowest M_w with 851 ± 6 g mol^{-1}, compared to 924 ± 3 g mol^{-1} for the MF/MeOH, 1042 ± 4 g mol^{-1} for the FA/water and 1182 ± 57 g mol^{-1} for the FA/MeOH conditions. As illustrated in Fig. 2, the FA/MeOH system produced higher M_w products than the MF/MeOH. Higher molecular weight lignin fragments are thought to be more predisposed to charring. As a consequence, the high amount of char produced in the case of the MF/MeOH could reduce the presence of high molecular weight product in the oil. In other words, the condensation of the lignin, favoured in absence of water, could lead to an initial increase of the M_w of the lignin oil. Then the higher molecular weight fragments in the oil may partake in char forming reactions (also favoured in absence of water) leading to a lowering of the M_w of the final lignin oil. Many studies give evidence for the more highly aromatized and/or the more conjugated compounds in coal and biomass derived oils being more reactive towards char formation – these compounds are often the higher molecular weight components.[30,31]

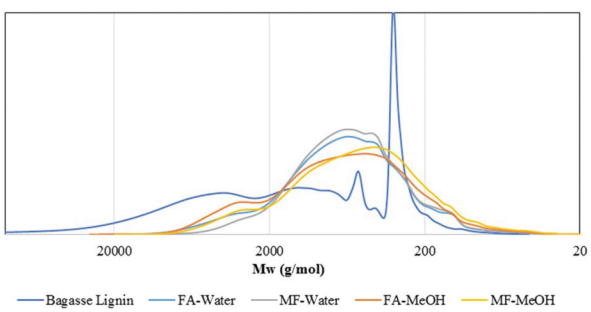

Fig. 2 Size exclusion chromatograms of the initial bagasse lignin and oil fractions after lignin depolymerization as a function of the experimental conditions.

Monomer distribution and yield of the oils. The quantification of the dichloromethane soluble products of the lignin oil is illustrated in Table 3 and Fig. 3. According to NMR analysis, the syringyl unit was the main constituent of the bagasse lignin. However, as illustrated in Fig. 3, syringol was only detected in the methanol system and it contributed to less than 0.21 or 0.75 g per 100 g of oil for FA/MeOH and MF/MeOH respectively. The absence of syringol under other conditions could be explained by its demethoxylation to produce guaiacol. It can be suggested that the observed monomers were mainly produced from ferulic acid (G-type units) and *p*-coumaric acid (H-type units) instead of the syringyl backbone of the lignin.

The distribution of the different products was highly dependent on the nature of the solvent. Under aqueous conditions, phenols and catechols were the main products. The distribution was more diverse when methanol was used with a significant presence of anisoles, suggesting that the phenolic hydroxyl groups were methylated. On the other hand, guaiacol was present in a higher concentration when methanol was used, compared to the aqueous system. This can be explained by the hydrolysis of the methoxy group to produce catechols in the presence of water. The methanol medium favoured the methylation of the phenolic hydroxyl, while the aqueous medium favoured the demethylation of the methoxy group. Methane was not detected in the FA/water system (Fig. 7). It is suggested that the methoxy group of the lignin undergoes hydrolysis to produce catechol and methanol rather than undergoing reductive cleavage to generate methane. This

Table 3 Quantitative GC-MS analysis of the monomeric products

	FA-water		MF-water		FA-MeOH		MF-MeOH	
	g per 100 g of oil	g per 100 g of lignin	g per 100 g of oil	g per 100 g of lignin	g per 100 g of oil	g per 100 g of lignin	g per 100 g of oil	g per 100 g of lignin
Anisole	0	0	0	0	0	0	0.10	0.06
2-Methylanisole	0	0	0	0	0	0	0.06	0.03
4-Methylanisole	0	0	0	0	0.13	0.10	0.28	0.16
Phenol	1.70[a]	1.34[b]	1.44	1.19	0.3	0.25	0.26	0.15
4-Ethyanisole	0	0	0	0	0.93	0.76	1.42	0.82
2-Cresol	0.07	0.05	0.08	0.06	0.12	0.09	0.14	0.08
1,2-Dimethoxybenzene	0	0	0	0	0.23	0.19	0.35	0.2
4-Cresol	0.4	0.31	0.36	0.3	0.15	0.12	0.13	0.07
Guaiacol	0.08	0.06	0.3	0.25	0.64	0.52	0.64	0.37
4-Ethylphenol	2.03	1.59	2.05	1.7	0.78	0.64	0.66	0.38
4-Methylguaiacol	0.02	0.01	0.17	0.14	0.99	0.81	0.91	0.53
Cyclohexane-1,2-diol	0.13	0.1	0.24	0.2	0	0	0	0
1,2,3-Trimethoxytoluene	0	0	0	0	0	0	0.2	0.11
catechol	1.19	0.93	1.02	0.85	0.15	0.12	0.16	0.09
4-Propylphenol	0.1	0.08	0.07	0.06	0	0	0	0
4-Methylcatechol	0.42	0.33	0.45	0.38	0.06	0.05	0.03	0.02
3-Methylcatechol	0.14	0.11	0.16	0.13	0.06	0.05	0.02	0.01
4-Ethylguaiacol	0.01	0.01	0.19	0.16	0.76	0.62	0.71	0.41
Syringol	0	0	0	0	0.12	0.1	0.59	0.34
4-Ethylcatechol	0.7	0.55	0.92	0.76	0.16	0.13	0	0
Methyl-ethylguaiacol[c]	0.1	0.08	0.12	0.1	0.07	0.06	0	0
4-Propylguaiacol	0	0	0	0	0.23	0.19	0.16	0.09
3-Methoxycatechol	0	0	0	0	0.05	0.04	0.07	0.04
4-Methylsyringol	0	0	0	0	0.04	0.03	0.17	0.1
Ethyl-methylcatechol[c]	0.1	0.08	0.12	0.1	0.07	0.06	0	0
4-Propylcatechol	0.27	0.21	0.35	0.29	0.06	0.05	0	0
pyrogallol	0.01	0.01	0	0	0	0	0	0
5-Methyl-3-methoxycatechol	0	0	0	0	0.08	0.06	0.06	0.03
4-Ethylsyringol	0	0	0	0	0.05	0.04	0.08	0.05
2-Phenol-ethanol	0.21	0.17	0.24	0.2	0	0	0	0
5-Ethyl-3-methoxycatechol	0	0	0	0	0.08	0.07	0.08	0.05
4-Propylsyringol	0	0	0	0	0.09	0.07	0.12	0.07
5-Propyl-3-methoxycatechol	0	0	0	0	0	0	0	0
Sum	7.66	6.01	8.28	6.87	6.40	5.22	7.40	4.27

[a] g per 100 g of oil. [b] g per 100 g of the Klason lignin content of the bagasse lignin. [c] Specific isomer unidentified.

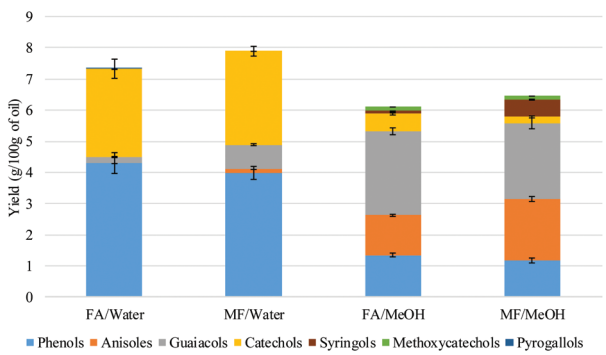

Fig. 3 Quantitative GC-MS analysis of the monomeric products (g per 100 g of oil).

could not be confirmed in this study as methanol is lost during the product recovery step and would be accounted for in the unrecovered fraction. Etherification under methanol conditions or ether hydrolysis in the aqueous system explain the difference in carbon content derived from the sum of char + oil determined by elemental analysis (Table 2) and also the lower amount of unrecovered fraction in the case of the methanol system (Fig. 1). Previous studies also highlighted the alkylation of the aromatic ring of the lignin when the reaction was conducted in alcoholic media.[20,21] In the present study, no significant alkylation of the aromatic ring was observed, although some alkylation did occur. This could be explained by the lower reaction temperature used in the present study.

Onwudili reported the production of up to 15% of alkylated benzene and up to 10% of alkylphenols when the lignin was two-stage depolymerized at 265 °C for 1 h followed by 350 °C for 5 h. When the reaction was conducted at 265 °C for 5 h and 350 °C for 1 h, phenol was the main product accounting for up to 18% of the lignin feed.[19] Elsewhere it has been reported that catechol was produced when the reaction was conducted at 265 °C for 6 h.[12] In the present study, no alkylated benzene products were detected under our reaction conditions. The deoxygenation of the aromatic ring probably requires a higher temperature than used in the present study (300 °C).

Time course study of the lignin transfer hydrogenation

Evolution of the oxygen contents and molecular weight of the oil. For the depolymerization study of lignin as a function of time, lignin was reacted in the presence of MF and water (Table 7). The mass of each type of atom contained in the oils can be calculated by taking into account the yield of oil generated after different reaction times and the elemental composition of the oil. For example, from 100 g of bagasse lignin containing 59 g of carbon and 32 g of oxygen, 76 g of oil was produced after a 4 h reaction containing 56 g of carbon and only 12 g of oxygen. As illustrated in Fig. 4, CHN analysis of the oil recovered after different reaction times showed that the mass of recovered carbon increased from 59 g to 68 g at the early stage of the reaction (up to 270 °C) suggesting that the formate reacted with the lignin. However, the fact that the mass of oxygen did not increase suggests that lignin deoxygenation had already started and balanced the amount of oxygen incorporated from the formate molecules. The mass of hydrogen also increased from 5.8 to 8.6 wt% and then decreased slightly to 6.6 wt% after 4 h of reaction. While the mass of oxygen decreased from 32.4 to 12.2 wt% from the bagasse lignin to the oil generated after 4 h of reaction, the mass of carbon only decreased from 59.2 to 56.0 wt%.

As illustrated in Fig. 5, the depolymerization of the bagasse lignin already occurred before the reaction temperature reached 270 °C. The NMR analysis (Fig. S.1†) of oil produced once the temperature reached 270 °C showed that the alkyl–aryl ether linkages had already disappeared at this stage of the reaction. Cleavage of the alkyl–aryl ether linkage occurred during the temperature ramp. However, the region of the aromatic proton could still be distinguished between the guaiacyl and syringyl units. On the other hand, the correlation peak related to the coumarate and ferulate structure disappeared while a correlation peak appeared next to the $H_{2,6}$ signal of the hydroxyphenyl lignin unit. This peak could be attributed to the production of alkylphenols such as ethylphenol.

As illustrated in Fig. 5, the M_w of the oil then slowly decreased to 880 g mol^{-1} after 4 h reaction before increasing to 1070 g mol^{-1} at 6 h. The small increase between 4 and 6 h may be attributed to condensation reactions.

Evolution of monomers: yield and product distribution. The evolution of the monomer quantity and type was measured as a function of time. As illustrated in Fig. 6, the yields of the monomers steeply increased during the temperature ramp between 270 and 285 °C from 4.4 to 9.6 wt% of bagasse lignin. Then, the yields started decreasing as the reaction temperature approached 300 °C. While the oxygen content and the M_w of the lignin oil decreased with increasing reaction time, the yields of identified monomers significantly decreased. The selectivity of monomers, (as defined in the Experimental section) also changed significantly betweeen 270 °C and 30 min reaction time at 300 °C. The syringols type molecules which were major products at 270 °C totally disappeared after 10 min reaction at 300 °C. The NMR analysis of the oil produced after 4 h reaction confirmed the disappearance of the S-type units (Fig. S.1.C†). Even if it is difficult to corrleate the lignin structure to the aromatic proton of the spectrum, the total absence of the $S_{2,6}$ correlation peak suggested substantial degradation or modification of the S-type units of the lignin. This could be explained by the demethylation of the syringol to methoxycatechols and pyrogallols. Then, the low stability of the pyrogallol could lead to the disappearance of the syringyl (S)-type units derived products (syringols, methoxycatechols, pyrogallols) after 30 min reaction. On the other hand, the yield of catechols and guaiacol, reached a maximum after 10 min reaction with 2.2 and 1.7 wt% and then decreased to less than

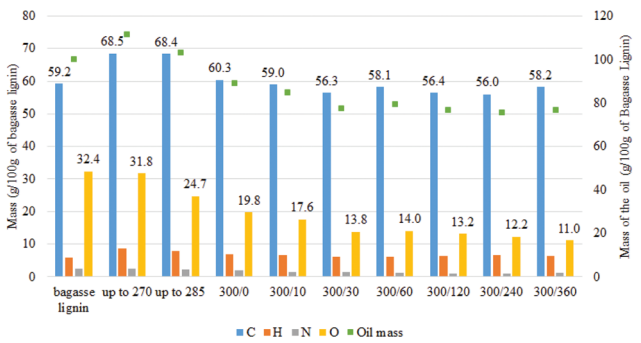

Fig. 4 Evolution of the mass of each type of atom in the oil produced at different reaction time based on 100 g of starting bagasse lignin [300/0: temperature (°C)/time (min)].

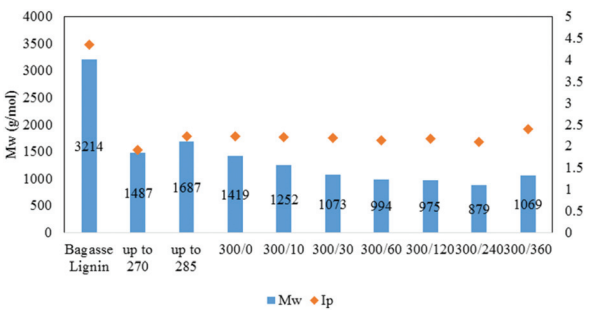

Fig. 5 Weight-average molecular weight and index of polydispersity of the lignin oil as function of the reaction time [300/0: temperature (°C)/time (min)].

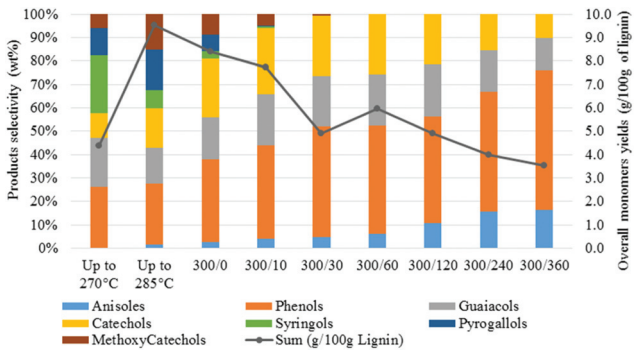

Fig. 6 Monomers yields and selectivity as function of the reaction time [300/0: temperature (°C)/time (min)].

0.4 and 0.5 wt% after 6 h reaction. The stability of the phenols (H-type lignin units) was highlighted by the increase of the H-type unit product selectivity from 26 wt% at 270 °C to 76 wt% after 6 h reaction. Higher stability of the phenols under operating conditions compared to the catechols and pyrogallols could explain the evolution of the product selectivity toward the H-type unit derived monomers (phenols and anisoles). As observed in the methanol media experiment, the production of anisoles could be attributed to the methylation of the phenol with methanol. In that case, the methanol came from the hydrolysis of the MF as well as the demethylation of the phenolic hydroxyl. This also illustrates the competitive reactions between demethylation and methylation of phenolic hydroxyl group. The presence of guaiacol type molecules after several hours of reaction could also be explained by the same equilibrium between demethylation and methylation of the phenolic hydroxyl group. Unlike pyrogallol, it can be suggested that the relative stability of the catechols prevented the total disappearance of the G-type unit derived products, even if the relative selectivity decreased from 50 wt% after 10 min to 24 wt% after 6 h reaction.

A close analysis of the product distribution highlighted that the H-type units were more stable that the G-type and S-type units. As a consequence, higher monomers yields should be expected from H-rich lignin. On the other hand, the S-rich lignin (usually dominant in grasses and hardwood) did not seem to be the most suitable lignin structure for transfer hydrogenation reactions in aqueous media.

Gas compositions after reaction

Effect of the reagent system. Given previous studies, it was anticipated that the reaction gas composition will affect the lignin depolymerization and condensation.[21] In this part of the study, the role of the gaseous environment on the lignin depolymerization was examined. According to a previous study, the decomposition of FA in presence of water can follow (b) decarboxylation (E_a = 45.3–47.9 kcal mol^{-1}) or (c) decarbonylation (E_a = 49.9–55.4 kcal mol^{-1}) pathways (Scheme 1).[25] Theoritical work also showed that MF could also be decomposed *via* (d) decarbonylation (E_a = 74.8 kcal mol^{-1}), (e) decarboxylation (E_a = 86.5 kcal mol^{-1}) or (f) formaldehyde pathways (E_a = 80.3 kcal mol^{-1}).[32]

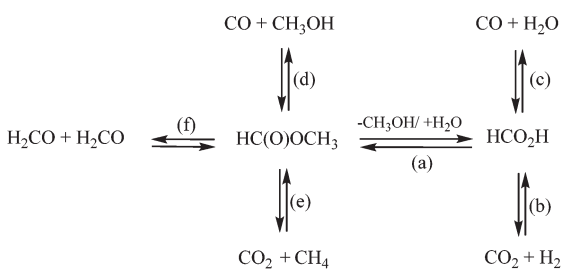

Scheme 1 Reaction pathways of formic acid and methyl formate equilibrium and decomposition [(a) equilibrium between formic acid and methyl formate; (b, e) decarboxylation or (c, d) decarbonylation, (f) formaldehyde decomposition pathways].

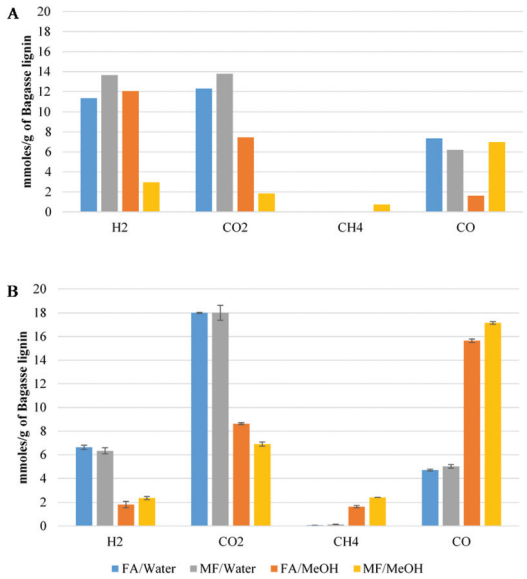

Fig. 7 Gas composition of formic acid/methyl formate decomposition without (A) or with (B) the presence of bagasse lignin (mmol g^{-1} of bagasse lignin).

Fig. 7 shows the gas composition after decomposition of FA/MF without (A) or with (B) lignin. For comparison, the same number of moles of MF or FA was used for both sets of experiments (A & B) and the gas concentrations were reported as a function of the mass of lignin. As illustrated in Fig. 7A, all the FA/MF were decomposed in the aqueous system after 4 h reaction in the absence of lignin. On the other hand, the sum of CO + CO_2 showed that less than 50% of the FA/MF was decomposed when methanol was used. This is explained by the higher stability of methyl formate towards decomposition. Indeed, the activation energy for the decarbonylation of the MF was previously estimated to be 74.8 kcal mol^{-1} while the FA carboxylation activation energy can be as low as 45.3 kcal mol^{-1}.[25,32] As illustrated in Scheme 1, the hydrolysis of the MF in water generated the FA which then decomposed *via* decarboxylation or decarbonylation pathways to produce CO_2 an H_2 or CO, respectively.[33] The gas composition was similar when excess water was used (FA/W or MF/W). On the other hand, the gas composition after decomposition of the FA (FA/MeOH) or methyl formate (MF/MeOH) was different. For the FA/MeOH system, the molar ratio CO_2/CO was 4.5 whilst in the MF/MeOH case, the ratio was 0.22. It is also interesting to note that the ratio of H/CO_2 was 1.6 in methanol whilst it was close to 1 under aqueous conditions. The higher production of hydrogen could be explained by the methanol reforming reaction. As illustrated in Fig. 7B, the presence of lignin significantly modified the gas composition and catalysed the decomposition of FA/MF in methanol. However, the catalytic effect of lignin was unclear and further analysis is required to understand if, for example, metal impurities (if present) or lignin itself are the reason for this effect. The gas composition in the presence of lignin was also highly affected by the

solvent used in the depolymerization experiments, rather than the transfer hydrogenation agent. In the water system, CO_2 was the most abundant gas with 18 mmol g^{-1} of lignin. The greatest CO yield was observed under both methanol systems (FA/MeOH and MF/MeOH), with 15.6 mmol and 17.2 mmol g^{-1} of bagasse lignin respectively. The decarboxylation of FA appears to be the main decomposition pathways in aqueous media, and decarbonylation of FA and MF under non-aqueous media which is in agreement with a previous study.[25] In aqueous media, the fast hydrolysis of the MF to FA will significantly exacerbate the MF decomposition.[33]

Methane was only produced in significant quantities in the non-aqueous medium and is likely to come from hydrogenation of methanol and/or decarboxylation of MF (Fig. 4A). Under aqueous reaction conditions, the low amount of methane suggests that the demethylation of the methoxy group proceeds *via* a hydrolysis mechanism instead of hydrogenolysis. The number of moles of MF or FA used for the experiment were 20 mmol g^{-1} of lignin. The sum of CO_2 + CO produced in all four experiments ranged from 22.7 mmol to 24.3 mol for FA/water and FA/MeOH conditions respectively. These values are slightly higher than the total amount of carbon oxides generated by the decomposition of the FA and can be partially explained by the decarboxylation of the *p*-coumaric acid and ferulic acid of the lignin. According to the NMR result, decarboxylation of both cinnamic acids should generate less than 1 mmol of CO_2 per gram of lignin. However, this could be overstated due to the overestimation of the *p*-coumaric acid and ferulic acid using analysis *via* NMR. On the other hand (Table 4), the blank experiment, where bagasse lignin was only reacted in the presence of water, at 35 bar-g nitrogen, produced 3 mmol of CO_2 per g of lignin which is in agreement with the overproduction of CO_2. Compared to the water system, the total carbon oxides was also slightly higher in the methanol system and could be explained by the methanol reforming reaction. It is well known that formaldehyde is produced during acid-catalyzed hydrolysis of lignin. In addition to being involved in lignin condensation, the formaldehyde can disproportionate to give methanol and FA (Scheme 1) or cross-disproportionate with FA to give CO_2 and methanol.[34] As a consequence, the degradation pathway of the formaldehyde could also account for the overproduction of CO_2.

In the system without lignin (Fig. 7A), the H_2/CO_2 ratio was in all cases equal to or greater than one. However, as illustrated in Fig. 7B, the difference of moles between hydrogen and carbon dioxide can be explained by the direct or indirect involvement of hydrogen in the deoxygenation of lignin. As illustrated in Fig. 7B, taking into account the CO_2 coming from the lignin (3 mmol g^{-1}, Table 5), around 8.5 mmol of hydrogen per gram of lignin were consumed in the water system while only 3.8 and 1.5 mmol were consumed when non-aqueous conditions were applied. The higher consumption of hydrogen could be correlated to less char formation due to fewer lignin condensation reactions.

Gas evolution as function of the time. In the previous section the gas composition after reaction suggested that a significant amount of hydrogen was consumed by the lignin. To the best of the authors' knowledge, there are no previous time-course studies on the gas composition during the transfer hydrogenation of lignin. The composition of the evolving gases should be helpful to explain the FA/MF decomposition mechanism and the role of reactive gas species (*e.g.* CO or H_2). As illustrated in Table 4, the sum of CO_2 + CO showed that the decomposition of the FA/MF occurred at an early stage to produce three times more moles of CO_2 than H_2. After 10 min of reaction, the sum of CO + CO_2 reached a maximum of 21 mmol g^{-1} then remained constant. However, once the temperature of the reaction reached 300 °C, the amount of CO decreased to 0.053 mmol min^{-1} between 30 to 360 min while the increase of CO_2 was inversely proportional, increasing to

Table 4 Gas composition of the reaction as function of the reaction time (mmol g^{-1} of lignin) [300/0: temperature (°C)/time (min)]

	H_2	CO_2	CH_4	CO	CO + CO_2	CO_2–H_2
Up to 270 °C	1.9	6.3	0.0	8.7	15.0	4.5
Up to 285 °C	3.5	9.2	0.0	10.7	19.9	5.7
300/0	3.1	9.3	0.1	11.1	20.4	6.2
300/10	4.5	10.9	0.1	10.1	21.0	6.4
300/30	4.0	10.6	0.2	10.1	20.7	6.6
300/60	3.8	11.3	0.3	9.6	20.9	7.5
300/120	4.1	12.8	0.4	8.4	21.2	8.7
300/240	4.5	14.1	0.8	8.0	22.1	9.7
300/360	4.9	14.7	1.1	7.0	21.7	9.8

Table 5 Gas composition and yields after reaction for different experimental conditions

		Gas composition (mmol g^{-1} of lignin)					Yields (g per 100 g of lignin)		
Entry	Conditions[a]	H_2	CO_2[b]	CH_4	CO	CO_2–H_2	Char	Oil	Unrecov.
1	N_2	0.0	3.0	0.1	0.1	3.0	34	37	33
2	CO-blank	0.7	0.6	0.0	27.8	−0.1	n.a.	n.a.	n.a.
3	CO-10 bar	1.2	4.8	0.1	4.1	3.6	18	49	33
4	CO-20 bar	2.4	6.9	0.1	9.4	4.5	11	57	33
5	CO-35 bar	4.4	10.0	0.1	18.2	5.6	6	63	31
6	H_2/CO	14.5	0.5	0.0	8.8	n.a.	31	42	28
7	H_2	21.0	0.1	0.1	0.1	n.a.	28	44	28

[a] See to Table 1 for experimental conditions. [b] CO_2 value in entries 3 to 7 are corrected with the amount of CO_2 generated from the lignin (entry 1).

0.073 mmol min^{-1} during the same period of time. This observation suggests that the CO was oxidized to CO_2 and somehow contributed to the deoxygenation of the lignin. A previous study reported that the water–gas-shift (WGS) reaction was observed at this temperature range in the absence of a catalyst.[24] In the present study it is unlikely that this phenomenon was only due to the WGS reaction as the hydrogen increased by only 0.02 mmol min^{-1} between 30 min and 360 min. Or, as illustrated in Table 4, the difference between CO_2 and H_2 increased with the reaction time. This result is in contrast with previous work on the conversion of hardwood lignin under 500 psi of carbon monoxide (cold pressure). The authors did not observe the oxidation of the carbon monoxide to carbon dioxide when the reaction was conducted at 365 °C *i.e.* subcritical water.[22]

As illustrated in Fig. 4, methane was a significant product when methanol conditions were used. In the water system, methane was produced at a constant rate of 0.017 mmol min^{-1}. This could come from the methanol generated by the demethylation of guaiacol and syringol. Methane is also likely to come from direct hydrogenation of methanol and/or from the carbonylation of methanol with CO followed by decarboxylation of MF.

The time-course study of the gas composition showed that carbon monoxide was consumed while CO_2 was generated. As the FA was decomposed at an early stage of the reaction, the presence of carbon monoxide and hydrogen had to play a critical role in the prevention of lignin recondensation. This aspect of the transfer hydrogenation using FA is often ommitted and will be discussed in the next section.

Depolymerization of bagasse lignin in presence of reductive gas. To understand the effect of carbon monoxide, additional experiments were performed where FA was substituted with CO and/or H_2. As illustrated in Table 5, the blank experiment without lignin (entry 2) generated a small amount of hydrogen and showed that the WGS reaction only occurred to a low extent. The low catalytic activity of the metal reactor wall could partially explain the WGS reaction. According to previous work, the catalytic effect of the metal reactor wall was observed from temperatures as low as 600 K in plug-flow-reactor configuration, with "substantially enhanced rates of reaction" for a metal-walled reactor *versus* quartz reactors.[35] The presence of lignin (entry 5) significantly increased the amount of hydrogen produced suggesting that the bagasse lignin appears to catalyze the water–gas shift reaction although the reason for this is unclear and may be related to the presence of ash components. As observed in the time course data, there is a an unbalanced amount between the CO_2 and H_2 (entries 3 and 4).

In order to check if the molecular hydrogen could be directly consumed during the experiment, lignin was reacted in the presence of a gas mixture composed of 20 bar-g (13.5 mmol g^{-1} of lignin) H_2 and 10 bar-g (8.6 mmol g^{-1} lignin) CO. As illustrated in Table 5 (entry 6), molecular H_2 was slightly produced, not consumed. This suggests that the hydridic proton from the formate, produced from CO and water, directly reacted with the lignin. This hypothesis has already been reported in previous work on hydrothermal liquefaction of a low-rank coal and biomass in the presence of carbon monoxide.[36,37] On the other hand, compared to entry 3 where half of the CO was consumed, barely any CO was consumed when the nitrogen was substituted with hydrogen. The presence of hydrogen appeared to inhibit the oxidation of CO to CO_2. The inhibition effect of the hydrogen could be explained by an equilibrium effect between hydrogen and carbon monoxide within the water–gas-shift reaction. The inhibition of the CO oxidation increased the char formation. As illustrated in Table 5, the char formation increased from 18% (entry 3) to 31% (entry 6) when nitrogen was substituted with hydrogen. In the pure hydrogen system (entry 7), the char formation was also much higher than in the carbon monoxide system (entry 5). This observation clearly shows that the molecular hydrogen is not active in the studied conditions and did not prevent lignin condensation reations.

As illustrated in Table 6, the oxygen content of the oil generated in the blank (entry 1) and under pure hydrogen (entry 5) were similar to the initial bagasse lignin (Table 1). No significant deoxygenation of the lignin oil was observed when the lignin was reacted in the presence of 35 bar-g nitrogen or 30 bar-g of hydrogen. On the other hand, the reduction of the oxygen content was significant in the char and was due to the carbonization of the lignin. The oils produced under CO conditions showed that their oxygen content decreases from 23.2 wt% to 20.2 wt% as the CO partial pressure increased from 10 to 35 bar-g. As illustrated in Fig. 8, there is a linear correlation between the lignin oil yields and the oxygen content of the oils. More deoxygenation of the lignin generated higher yield of oil. The deoxygenation of the lignin is a critical

Table 6 Elemental analysis of the oil and the char as a function of experimental conditions

		Oil (g per 100 g of oil)/[g per 100 g of lignin]				Char (g per 100 g of char)/[g per 100 g of lignin]			
#		C	H	N	O	C	H	N	O
1	N_2-35 bar[a]	61.0 [22.6]	6.7 [2.5]	3.3 [1.2]	29.0 [10.7]	77.0 [25.8]	5.2 [1.7]	3.0 [1.0]	14.8 [5.0]
2	CO-10 bar	66.5 [32.3]	7.3 [3.5]	2.9 [1.4]	23.2 [11.3]	79.1 [14.5]	5.8 [1.1]	3.0 [0.5]	12.1 [2.2]
3	CO-20 bar	68.6 [38.8]	7.4 [4.2]	3.1 [1.8]	20.9 [11.8]	79.3 [8.4]	5.8 [0.6]	3.0 [0.3]	11.9 [1.3]
4	CO-35 bar	69.3 [43.7]	7.4 [4.7]	3.1 [2.0]	20.2 [12.7]	79.3 [4.5]	6.6 [0.4]	2.8 [0.2]	11.2 [0.6]
5	H_2-30 bar	62.6 [27.4]	6.6 [2.9]	3.1 [1.4]	28.3 [12.4]	74.8 [21.1]	5.3 [1.5]	2.7 [0.8]	17.3 [4.9]
6	FA/W	71.2 [49.1]	8.0 [5.5]	2.7 [1.9]	18.2 [12.6]	70.9 [0.9]	6.1 [0.1]	2.3 [0.1]	20.7 [0.2]

[a] See to Table 1 for experimental conditions; values in g per 100 g of oil and [g per 100 g of lignin] were shown.

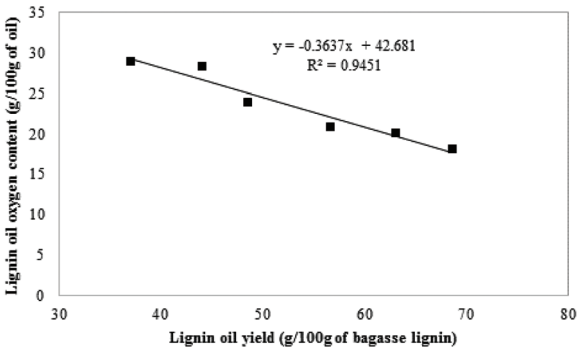

Fig. 8 Correlation between the oxygen content and the yield of the oil.

step in order to prevent condensation reactions leading to the formation of char.

Transfer hydrogenation of lignin model compounds with deuterated formic acid. To gain insight into the decomposition mechanisms occurring during the non-catalytic transfer hydrogenation of lignin, model compounds simulating the benzyl hydroxyl function were reacted in the presence of four combinations of FA or deuterated formic acid (*d*-FA) and water or deuterated water (D_2O). For simplification, only the products of the *d*-FA/H_2O conditions are shown in Scheme 2. A comparison of the ethylguaiacol mass spectra as a function of experimental conditions is shown in Fig. 9.

As illustrated in Fig. 9, the mass spectrum of ethylguaiacol suggests the incorporation of one deuterium to the benzylic position when the α-methylvanillyl alcohol was reacted with *d*-FA. In the presence of D_2O (Fig. 9C & D), the molecular mass of the ethylguaiacol increased to 230 g mol^{-1} and 231 g mol^{-1} without and with the presence of *d*-FA, respectively. As reported in a previous study, the incorporation of deuterium on the β-carbon of the alkyl chain, and on the aromatic rings, was attributed to the H/D exchange of D_2O in subcritical conditions.[38] The H/D exchange at the β-carbon position of the side chain is thought to proceed *via* a vinylguaiacol intermediate as shown in Fig. S.2.† The H/D exchange of the three protons on the β-carbon was confirmed by the loss of *m*/*z* 18 from the ethylguaiacol fragmentation (Fig. 9). However, the low electron density of the benzylic position could explain the absence of H/D exchange at this position. When comparing the cracking pattern of the product obtained from the reaction with *d*-FA and H_2O (B) to the pattern from *d*-FA and D_2O (D), the loss of 15 *m*/*z* (Fig. 9B) instead of 18 *m*/*z* (Fig. 9D) confirmed the absence of deuterium incorporation at the beta

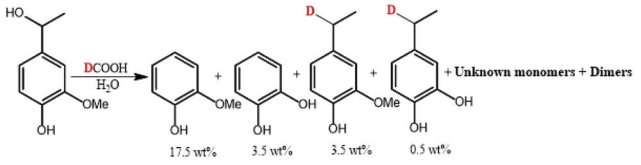

Scheme 2 Transfer hydrogenation of alpha-methyl vanillyl alcohol with formic acid-*d* [300 °C, 10 min].

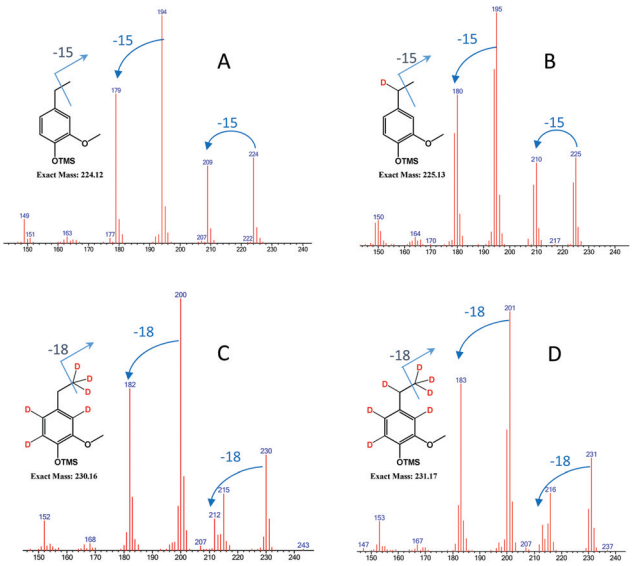

Fig. 9 GCMS spectrum of deuterated ethylguaiacols obtained from different conditions [experimental conditions: (A) FA/H_2O; (B) *d*-FA/H_2O; (C) FA/D_2O; (D) *d*-FA/D_2O].

carbon position of the alkyl chain under *d*-FA H_2O conditions (B). Ergo, in case (B) the deuterium has to be incorporated at the alpha position. Therefore, the incorporation of deuterium on the benzylic position can only be attributed to the transfer hydrogenation of the deuterated formic acid (DCOOH). Under these conditions, the mass spectrum also showed the presence of ethylguaiacol (*m*/*z* = 224) without deuterium incorporation (Fig. 9B). The reduction of the α-methylvanillyl alcohol to ethylguaiacol does not necessarily require the presence of FA suggesting that other hydride sources can be involved in the reductive reaction. Indeed, in the blank system (*i.e.* no FA), the production of ethylguaiacol was observed and could be explained by the transfer hydrogenation of the α-methylvanillyl alcohol in order to generate acetoguaiacol and ethylguaiacol. Another reason for the production of ethylguaiacol under blank conditions could be due to the involvement of acetaldehyde. The production of acetaldehyde could be attributed to the retro aldol reaction leading to the generation of guaiacol, which has been observed as the main product here. Even if the role of acetaldehyde in the reduction has not been clearly identified, previous authors reported that the disproportionation of acetaldehyde can generate carbon monoxide.[39] The carbon monoxide could then react with water to produce an active reducing reagent. Acetaldehyde could also be a precursor to a hydride reagent and indirectly reduce the α-methylvanillic alcohol to ethylguaiacol.

The benzylic position of the lignin is well-known for being one of the main lignin positions where condensation can occur. The reduction of the benzylic hydroxyl *via* transfer hydrogenation will limit condensation reactions. Further evidence of the importance of the benzylic position and oxygen in condensation reactions comes from research on the production of synthetic pitches from coal tar derived anthracene

oil.[31,40,41] In that work anthracene oil was air blown at 280–300 C in the presence of an iron chloride catalyst. It was found that the incorporation of oxygen groups into aromatic side chains of the anthracene oil molecules was important for improving the yield of higher mass compounds (500 to >3000 amu) compared to nitrogen blown conditions. It was determined that oxygen plays an important role in enhancing condensation reactions between small polyaromatic hydrocarbons. Lignin condensation reactions could be limited in the presence of FA *via* the reduction of benzylic hydroxyl groups *via* transfer hydrogenation.

General discussion. Based on the described findings, the transfer hydrogenation of lignin in the presence of MF, FA and carbon monoxide is posited to proceed as in Fig. 10; an equilibrium is established in the presence of H_2O leading to all three reactive species being present in the reaction mixture, as shown in Scheme 1. As illustrated in Fig. 10, the more stable MF could be seen as a storage molecule for the hydridic proton of FA. As a consequence, the use of MF could delay the release of FA and avoid complete consumption of FA during the early stages of the reaction. The FA is consumed *via* pathway A[34,42] or *via* direct decomposition to carbon monoxide (pathway B) or carbon dioxide (pathway C). Then, it is suggested that the CO is converted to formate (FA) in the presence of lignin and water (pathway D) which prevents carbonization of the lignin. Under subcritical water conditions, the ability of carbon monoxide to activate the hydrogen of water *via* the formation of formate has been previously reported.[36] Finally, the deuterated experiment confirmed the transfer hydrogenation of a lignin type molecule at the benzylic position which is a key step for preventing lignin condensation. Unlike previous studies,[21] this study demonstrates that FA reacts directly with the lignin *via* transfer hydrogenation without the formation of molecular hydrogen. According to previous work, the bond dissociation energy of the hydride of the formate was measured as 90.8 kcal mol^{-1} while for molecular hydrogen it is 104 kcal mol^{-1}.[43] The lower bond dissocation energy of the formate compared to molecular hydrogen could explain its reactivity. Under our experimental conditions, molecular hydrogen did not contribute to the deoxygenation of the lignin (pathway E).

It is clear that the presence of formate or CO alone helped to limit char formation. Even if the CO conditions minimized the char formation, better results were achieved when using formate/water. In the presence of formate, the higher deoxygenation of the oil at early stages of the reaction may be the key to the minimization of the condensation reactions which lead to char formation. In the present study, FA was shown to be quickly consumed during early stages of the reaction. Nearly all the FA/MF was reacted or decomposed before the reaction temperature reached 300 °C. At high lignin loading, a significant partial pressure of carbon monoxide (relative to 21 bar-g of cold pressure) was generated from MF/FA decomposition once the reaction temperature reached 300 °C. This high CO partial pressure combined with an aqueous media limited condensation reactions between lignin fragments (Table 5, entries 3–5). Also, even if the partial pressure of CO (cold pressure) was reduced to 14 bar-g after 6 h of reaction, it was still high enough to prevent significant carbonization of the lignin (less than 2% char). However, in the non-aqueous system, the presence of carbon monoxide was not useful due to the absence of water and did not prevent the formation of char as illustrated by the MF/MeOH results. The possibility of using carbon monoxide in an aqueous media as a transfer hydrogenation reagent is a promising way to reduce the FA loading and to improve the environmental credentials (by using water instead of an organic solvent) and the economics of the process. On the other hand, conversion of carbon monoxide to active formate (FA) is slow which is less desirable. As previously reported, activation of the carbon monoxide with a promoter like sodium formate or sodium carbonate led to a better oil yield and less char formation.[23,36] However, the addition of promoter will also increase the water–gas-shift type reaction and generate unreactive hydrogen.

It is interesting to note that the conversion of the FA to hydrogen, under the conditions outlined above, could be classified as a parasitic reaction. In other words, carbon monoxide which is usually poisonous for metal catalysts appears to be the main contributor to the depolymerization of lignin and limits char formation under non-catalytic conditions.

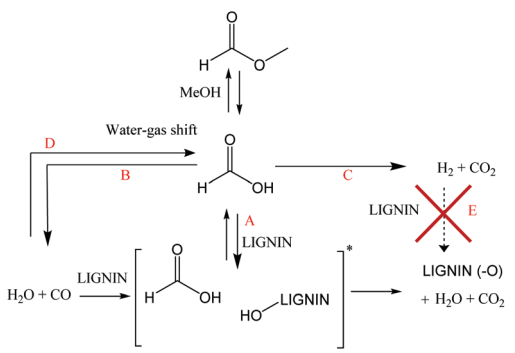

Fig. 10 Posited mechanism for the deoxygenation of lignin using formate or CO [*hypothetical interaction between CO, water and lignin].

Experimental

Materials

All chemicals were reagent grade and purchased from Sigma-Aldrich (St Louis, MO), unless otherwise noted. Bagasse lignin cake was obtained from the saccharification residue of the diluted acid pretreated sugarcane bagasse. On a dry basis, the lignin cake is composed of 35.7 wt% of Klason lignin, 39.5 wt% of glucan, 4.9 wt% of xylan and 1.6 wt% of ash. Hydrogen (UHP300), nitrogen (UHP300) were supplied from Airgas (Ragnor, PA) and carbon monoxide (99.5%) from Praxair (Danbury, CT). Dimethylsulfoxide-d_6 was purchased from Cambridge Isotope Lab (Tewksbury, MA).

Alkaline extraction of the saccharification residue

Due to the low lignin purity of the sugarcane bagasse saccharification residue, alkaline extraction of the lignin was performed. Wet lignin cake (187.5 g at 40% dry matter, 75 g of dry lignin cake) was mixed with 562.5 mL of DI water and 75 mL of 5 N NaOH in 2 L autoclave glass bottle. The bottles were loosely tightened, and the alkaline mixture was autoclaved at 121 °C (15 psi) for 1 h. After reaction, the mixture was cooled down to room temperature (RT) and centrifuged. The residue was washed 3 times with 250 mL of DI water. The alkaline liquors were combined together and cooled to 7 °C. Then, the liquor (pH = 12) was acidified with 6 N HCl up to pH 2–3 to precipitate the lignin. The acidic slurry was centrifuged, and the precipitate was washed three times with 250 ml of DI water. Finally, the purified/alkaline extracted bagasse lignin was dried at 45 °C under vacuum for 3 days and gently crushed using a mortar and pestle.

Bagasse lignin depolymerization

Formic acid and methyl formate systems. The lignin depolymerization was performed at 20 wt% lignin loading in the absence of a metal catalyst under four reagent/solvent scenarios as reported in Table 7. In duplicate, 4 g of bagasse lignin, 11.20 or 12.30 g of methanol or water and 4.80 g (20 mmol g^{-1} of lignin) of methyl formate or 3.68 g (20 mmol g^{-1}) of formic acid were added in 75 mL Parr vessel (Multiple Reactor System 5000). The reactor was sealed and purged four times with nitrogen (10 bar-g) and pressurized at 10 bar-g with nitrogen. Without stirring, the reaction temperature was increased up to 300 °C in 40 min, the pressure inside the reactor rapidly stabilized at 137 to 165 bar-g depending on the solvent used (Table 7). Even though no attempt to control the heating rate was made, 40 min was consistently required to reach 300 °C. At the end of an experiment the heater was shut down and the reactor allowed to cool to 150 °C before being placed in an ice bath until the reactor was at room temperature. The reactor reached room temperature in less than 60 min. Then, gas samples were collected during the degassing of the reactor. Using a two-digit scale, the mass of the product gases was obtained from the difference between the mass of reactor after degassing and the mass of the reactor before the nitrogen was introduced. The procedure was performed with care in order to minimize the error induced by the ice bath cooling and the water cooling system of the transducer. With a mass difference above 3.00 g, less than 3% variation in the gas yield was observed between two duplicate experiments.

$$\text{Mass of gas} = \text{mass of degassed reactor} - \text{mass of the loaded reactor (before pressurization)}$$

For collection of the oil, 40 ml of THF was added into the reactor to solubilize the oily fraction. The mixture was centrifuged and the residue (char) was washed twice with THF/MeOH (2/1: v/v). The oily product was recovered after solvent removal using a rotavapor (50 mbar at 35 °C) and the remaining water was co-evaporated with ethanol. The work-up procedure may involve the loss of some volatile lignin-derived products (*e.g.* anisole). The bulk of the "unrecovered fraction" is due to water, methanol, permanent gases and other volatile species that are lost during recovery of the oil.

Table 7 Experimental conditions for the depolymerization of lignin [MF: methyl formate; FA: formic acid; CO: carbon monoxide]

Reference	Lignin (g)	FA or MF (g)	Water or MeOH (g)	N_2 (bar-g)	Temperature (°C)	Time (min)	Working pressure (bar-g)
Reagents/solvent conditions							
MF/water	4.00	4.80	11.20	10	300	240	140.1
MF/MeOH	4.00	4.80	11.20	10	300	240	165.0
FA/water	4.00	3.68	12.32	10	300	240	137.3
FA/MeOH	4.00	3.68	12.32	10	300	240	160.5
Reaction time conditions							
MF/water-1	6.00	7.21	4.32	10	270	n.a.	108.7
MF/water-2	6.00	7.21	4.32	10	285	n.a.	143.6
MF/water-3	6.00	7.21	4.32	10	300	0	157.2
MF/water-4	6.00	7.21	4.32	10	300	10	164.8
MF/water-5	6.00	7.21	4.32	10	300	30	166.1
MF/water-6	6.00	7.21	4.32	10	300	60	163.5
MF/water-7	6.00	7.21	4.32	10	300	120	165.1
MF/water-8	6.00	7.21	4.32	10	300	240	166.1
MF/water-9	6.00	7.21	4.32	10	300	360	166.3

Reference	Lignin (g)	CO (g)/CO (bar-g)	Water (g)	N_2 or H_2 (bar-g)	Temperature (°C)	Time (min)	Working pressure (bar-g)
Gas conditions							
CO-blank	0	3.17/35	15	0	300	240	121.3
CO-10 bar	4.00	0.92/10	12.00	25	300	240	135.9
CO-20 bar	4.00	1.83/20	12.00	15	300	240	134.3
CO-35 bar	4.00	3.17/35	12.00	0	300	240	136.5
CO/H_2	4.00	0.92/10	12.00	20 (H_2)	300	240	95.0
N_2	4.00	0	15.00	35	300	240	128.9
H_2	4.00	0	15.00	30	300	240	99.1

The char was dried at 45 °C overnight and kept at room temperature. The oily fraction was dried in a desiccator under vacuum and stored at −20 °C.

Time-course study. It is expected that product distributions, selectivities and yields will change with reaction time, therefore a series of time-course experiments were conducted. The selectivity of a product category (*e.g.* phenolic compounds) as a function of the reaction time was given as the mass of an identified product category (*e.g.* phenolic compounds)/sum of the mass of all identified products. The protocol was the same except that 6 g of bagasse lignin (34 wt% loading), 7.21 g of methyl formate and 4.32 g of water were used. As illustrated in Table 1, two of the experiements were stopped before the temperature reached 300 °C. The time zero was set when the temperature of the reactor reached 300 °C. A time of 40 min was necessary to reach the working temperature. After reaction completion, the vessel was quickly cooled in an ice bath and the same workup procedure was performed as described previously.

Carbon monoxide and hydrogen experiments. For the experiments performed with carbon monoxide and hydrogen, 4 g of bagasse and 12 g of water were added into the reactor. Appropriate safety measures were taken in this study; it should be noted that if an industrial process based on this system were deployed, the safety of using CO would need to be considered. The vessel was then purged and pressurized using a mixture of CO/N_2 or CO/H_2. As illustrated in Table 7 (*e.g.* CO-20 bar-g), the reactor was purged and pressurized to 20 bar-g of carbon monoxide and then 15 bar of nitrogen was added to reach a total pressure of 35 bar-g. The time zero was set when the temperature of the reactor reached 300 °C and the reaction time at 300 °C was 4 h. After completion, the same workup procedure as described previously was employed. When only the CO and/or H_2 was added to the reactor, the mass of the gases produced from each experiment was determined as the difference between the mass of the reactor before and after degassing. When the nitrogen was added to the system (*e.g.* CO-10 bar), the mass of nitrogen introduced was subtracted from the mass of gases produced after reaction.

Transfer hydrogenation of deuterated formic acid on lignin model compounds. For the four deuterium experiments, 500 mg of α-methyl vanillyl alcohol was reacted in presence of 2 g of formic acid or formic acid-*d* (*d*-FA) and 15 ml of H_2O or D_2O at 300 °C for 10 min (FA/H_2O, *d*-FA/H_2O, FA/D_2O and *d*-FA/D_2O). After reaction, the products were extracted in ethyl acetate, silylated and analyzed by GCMS as described below.

HSQC 2D nuclear magnetic resonance. The two-dimensional (2D) ^{13}C–^{1}H heteronuclear single quantum coherence (HSQC) nuclear magnetic resonance (NMR) was performed as previously described.[44,45] Briefly, lignin or oil samples (~80 mg) were placed in NMR tubes with 750 μL DMSO-d_6. The samples were sealed and sonicated in a Branson 2510 table-top cleaner (Branson Ultrasonic Corporation, Danbury, CT), the samples appeared to fully dissolve under these conditions. The temperature of the bath was closely monitored and maintained below 50 °C. HSQC spectra were acquired at 398 K using a Bruker Avance-600 MHz instrument equipped with a 5 mm inverse gradient $^{1}H/^{13}C$ cryoprobe using the q_hsqcetgp pulse program (ns = 64, ds = 16, number of increments = 256, *d*1 = 1.0 s).[46] Chemical shifts were referenced to the central DMSO peak ($\delta C/\delta H$ 39.5/2.5 ppm). Assignment of the HSQC spectra is described elsewhere.[47] A semi-quantitative analysis of the volume integrals of the HSQC correlation peaks was performed using Bruker's Topspin 3.1 processing software.

Biomass compositional and elemental analysis. Klason lignin and carbohydrates contents of the Bagasse saccharification residue and alkali extracted lignin were performed as described in previous work.[45] All carbohydrates and lignin assays were conducted in duplicate. Elemental analysis of the dry lignin oil and char was performed on a CHNS 2400 PerkinElmer series II analyzer. The combustion was operated at 975 °C and the reduction of the nitrogen oxides to elemental nitrogen was operated at 680 °C. The gas mixture was separated by chromatography and quantified using a thermal conductivity detector. The acetanilide was used as standard for calibration. Accuracy of the instrument is 0.2–0.3% for C and N and 0.3–0.4% for H.

Gel permeation chromatography. The GPC analysis was performed on a Tosoh ECOSEC system, equipped with a UV detector (280 nm). A set of PS/DVB columns (5 μm, 300 × 7.5 mm, 50 Å and 500 Å, Polymer Lab) was used. The injection volume was 50 μL. The temperature of the column was 35 °C. The stabilized THF (250 ppm butylated hydroxytoluene BHT) was used as an eluent with a flow rate of 1 mL min^{-1}. Before injection, the oils or lignin were acetylated using pyridine/acetic anhydride mixture (1/1: v/v) overnight at room temperature. After acetylation, the reagent was removed under nitrogen gas stream at room temperature and traces of reagent were co-evaporated with ethanol. The acetylated oil or lignin were dissolved in THF (containing 250 ppm BHT) at a concentration close to 1 g L^{-1}. ECOSEC software was used to determine the molecular weight as a weight average molecular weight (M_w), the molecular weight as a number average molecular weight (M_n) and the index of polydispersity (IP). Molecular weight calibrations were obtained using polystyrene standards ranging from 162 to 29 150 g mol^{-1}. It should be noted that although GPC gives a good approximation of molecular weight for comparative purposes it does not provide absolute mass values for lignin type molecules. This is because the hydrodynamic radius and molecular structures of polystyrene and lignin molecules are likely to be quite different for molecules of similar mass.[48]

Gas analysis. The gas analysis was performed on a fuel-cell Shimadzu GC 2014 equipped with flame ionization and thermal conductivity detectors. Methanizer Kit was used in order to improve the detection sensitivity of the carbon monoxide and dioxide. The gas bag outlet was directly connected to the 1 mL loop system which was flushed with more than 20 mL of gas bag content. The quantification of hydrogen, carbon dioxide, carbon monoxide, methane, ethane, ethylene and acetylene was achieved using a customized standard gas mixture and a one-point calibration as recommended by the

instrument provider. The customized standard mixture was provided by Airgas and composed of 10 vol% carbon dioxide, 10 vol% carbon monoxide, 5 vol% hydrogen, 1 vol% methane and 0.1 vol% of ethane, ethylene and acetylene.

GC/MS analysis. GC/MS analysis of the catalytic conversion products was performed. An exact mass of oil products (Approx. 10.00 mg) were extracted with 300 μL of dichloromethane (DCM) containing the 1,3,5-tri-*tert*-butylbenzene as internal standard. An aliquot (5–10 μL) of the DCM soluble-products was silylated using 30 μL of pyridine and 70 μL of N, O-bis(trimethylsilyl)trifluoroacetamide (BSTFA). Qualitative and quantitative analyses were performed using an Agilent 6890N gas chromatography (GC) equipped with Agilent 5973N mass spectroscopy (MS). A DB-5MS capillary column (30 m × 0.25 mm × 0.25 μm) was used for this work. The quantification of the products was measured on the TIC using a set of reference compounds (listed in Table S.2†) with 1,3,5-tri-*tert*-butylbenzene as an internal standard.

Conclusion

The equilibrium system of formic acid, methyl formate and carbon monoxide in the presence of water has been evaluated, and the mechanism for the depolymerization/deoxygenation of lignin in the presence of formic acid or methyl formate at 300 °C has been elucidated. Formic acid is quickly decomposed to carbon dioxide or carbon monoxide, whilst the ratio between these two gases depends on the nature of the solvent. It was determined that hydrogenation of lignin using formic acid does not proceed *via* initial molecular hydrogen production, but rather *via* direct reaction of formic acid with lignin. This is also corroborated by the low ratio of molecular hydrogen and carbon dioxide observed.

Formic acid and carbon monoxide both contribute to lignin deoxygenation. In the absence of formic acid or carbon monoxide *i.e.* pyrolysis conditions in nitrogen, lignin oil contains high oxygen content and is more prone to carbonization. Deoxygenation of the lignin seems to be the critical step for limiting char formation.

With respect to oil and char formation, aqueous reaction conditions reduce the amount of char formation and lead to nearly complete demethylation of the lignin methoxy groups, thereby leading to catechol type molecules in the oil. The limited amount of char formation in the presence of water was attributed to the ability of carbon monoxide to activate the water molecule proton *via* the formation of formate. In the presence of lignin, carbon monoxide is converted to formate *via* a water–gas-shift type reaction. The formate prevents condensation of the lignin fragments thereby limiting char formation and producing more lignin products in the low molecular weight range.

Regarding depolymerization efficiencies, carbon monoxide has a lower efficiency than formic acid, arising from its role as a precursor to the active reducing reagent rather than carbon monoxide being the active reducing reagent itself. Using formic acid was more efficient due to a higher hydride concentration than in the carbon monoxide/water system. It is suggested that a combined process using formic acid and carbon monoxide would reduce the formic acid loading and provide a means for improving process economics.

Conflicts of interest

There are no conflicts to declare.

Acknowledgements

This work was part of the DOE Joint BioEnergy Institute (http://www.jbei.org) supported by the U.S. Department of Energy, Office of Science, Office of Biological and Environmental Research, through contract DE-AC02-05CH11231 between Lawrence Berkeley National Laboratory and the U.S. Department of Energy. The United States Government retains and the publisher, by accepting the article for publication, acknowledges that the United States Government retains a non-exclusive, paid-up, irrevocable, world-wide license to publish or reproduce the published form of this manuscript, or allow others to do so, for United States Government purposes. Total S.A. is kindly thanked for resources and support provided *via* the cooperative research and development agreement between LBNL and Total S.A. The authors thank Elena Kreimer for expert technical assistance.

References

1 V. Balan, D. Chiaramonti and S. Kumar, *Biofuels, Bioprod. Biorefin.*, 2013, **7**, 732–759.
2 R. Rinaldi, R. Jastrzebski, M. T. Clough, J. Ralph, M. Kennema, P. C. A. Bruijnincx and B. M. Weckhuysen, *Angew. Chem., Int. Ed.*, 2016, **55**, 8164–8215.
3 J. E. Holladay, J. J. Bozell, J. F. White and D. Johnson, *Top Value-Added Chemicals from Biomass-Volume II-Results of Screening for Potential Candidates from Biorefinery Lignin*, Pacific Northwest National Laboratory (PNNL), Richland, WA (US), 2007.
4 J. Zakzeski, P. C. A. Bruijnincx, A. L. Jongerius and B. M. Weckhuysen, *Chem. Rev.*, 2011, **110**, 3552–3599.
5 H. Zhang, R. Xiao, B. Jin, D. Shen, R. Chen and G. Xiao, *Bioresour. Technol.*, 2013, **137**, 82–87.
6 T. Wang, S. Qiu, Y. Weng, L. Chen, Q. Liu, J. Long, J. Tan, Q. Zhang, Q. Zhang and L. Ma, *Appl. Energy*, 2015, **160**, 329–335.
7 W.-C. Wang and L. Tao, *Renewable Sustainable Energy Rev.*, 2016, **53**, 801–822.
8 D. Verma, B. S. Rana, R. Kumar, M. G. Sibi and A. K. Sinha, *Appl. Catal., A*, 2015, **490**, 108–116.
9 S. Van Wesenbeeck, C. Higashi, M. Legarra, L. Wang and M. J. Antal, *Energy Fuels*, 2016, **30**, 480–491.

10 M. J. Antal Jr. and M. Gronli, *Ind. Eng. Chem. Res.*, 2003, **42**, 1619–1640.
11 S. Williams, C. Higashi, P. Phothisantikul, S. Van Wesenbeeck and M. J. Antal, *J. Anal. Appl. Pyrolysis*, 2015, **113**, 225–230.
12 J. A. Onwudili and P. T. Williams, *Green Chem.*, 2014, **16**, 4740–4748.
13 F. P. Bouxin, A. McVeigh, F. Tran, N. J. Westwood, M. C. Jarvis and S. D. Jackson, *Green Chem.*, 2015, **17**, 1235–1242.
14 A. L. Jongerius, P. C. A. Bruijnincx and B. M. Weckhuysen, *Green Chem.*, 2013, **15**, 3049–3056.
15 A. McVeigh, F. P. Bouxin, M. C. Jarvis and S. D. Jackson, *Catal. Sci. Technol.*, 2016, **6**, 4142–4150.
16 M. Oregui Bengoechea, A. Hertzberg, N. Miletić, P. L. Arias and T. Barth, *J. Anal. Appl. Pyrolysis*, 2015, **113**, 713–722.
17 A. Kloekhorst, Y. Shen, Y. Yie, M. Fang and H. J. Heeres, *Biomass Bioenergy*, 2015, **80**, 147–161.
18 U. Schuchardt, J. A. R. Rodrigues, A. Cotrim and J. L. M. Costa, *Bioresour. Technol.*, 1993, **44**, 123–129.
19 J. A. Onwudili, *Bioresour. Technol.*, 2015, **187**, 60–69.
20 C. Løhre, T. Barth and M. Kleinert, *J. Anal. Appl. Pyrolysis*, 2016, **119**, 208–216.
21 B. Holmelid, M. Kleinert and T. Barth, *J. Anal. Appl. Pyrolysis*, 2012, **98**, 37–44.
22 M. A. Hill Bembenic and C. E. Burgess Clifford, *Energy Fuels*, 2012, **26**, 4540–4549.
23 H. R. Appell, I. Wender and R. D. Miller, *ACS Div. Fuel*, 1969, **13**, 39–44.
24 Y. Yasaka, K. Yoshida, C. Wakai, N. Matubayasi and M. Nakahara, *J. Phys. Chem. A*, 2006, **110**, 11082–11090.
25 N. Akiya and P. E. Savage, *AIChE J.*, 1998, **44**, 405–415.
26 O. Jogunola, T. Salmi, J. Warna, J.-P. Mikkola and E. Tirronen, *Ind. Eng. Chem. Res.*, 2011, **50**, 267–276.
27 M. Kleinert and T. Barth, *Energy Fuels*, 2008, **22**, 1371–1379.
28 M. Kleinert, J. R. Gasson and T. Barth, *J. Anal. Appl. Pyrolysis*, 2009, **85**, 108–117.
29 J. Ralph, G. Brunow and W. Boerjan, in *Handbook of Plant Science*, John Wiley & Sons Ltd, 2007, vol. 2, pp. 1123–1132.
30 A. George, T. J. Morgan and R. Kandiyoti, *Energy Fuels*, 2014, **28**, 6918–6927.
31 T. J. Morgan and R. Kandiyoti, *Chem. Rev.*, 2014, **114**, 1547–1607.
32 J. S. Francisco, *J. Am. Chem. Soc.*, 2003, **125**, 10475.
33 T. Moriyoshi, K. Sam and Y. Uosaki, *High Pressure Res.*, 2001, **20**, 491–505.
34 G. Akgul and A. Kruse, *J. Supercrit. Fluids*, 2013, **73**, 43–50.
35 F. Bustamante, R. M. Enick, R. P. Killmeyer, B. H. Howard, K. S. Rothenberger, A. V. Cugini, B. D. Morreale and M. V. Ciocco, *AIChE J.*, 2005, **51**, 1440–1454.
36 M. Siskin, G. E. Phillips and S. R. Kelemen, US8500829B2, 2013.
37 I. T. Horvath and M. Siskin, *Energy Fuels*, 1991, **5**, 932–933.
38 M. Kubo, T. Takizawa, C. Wakai, N. Matubayasi and M. Nakahara, *J. Chem. Phys.*, 2004, **121**, 960–969.
39 Y. Nagai, S. Morooka, N. Matubayasi and M. Nakahara, *J. Phys. Chem. A*, 2004, **108**, 11635–11643.
40 P. Álvarez, M. Granda, J. Sutil, R. Menendez, J. J. Fernández, J. A. Viña, T. J. Morgan, M. Millan, A. A. Herod and R. Kandiyoti, *Energy Fuels*, 2008, **22**, 4077–4086.
41 J. Bermejo, A. L. Fernández, M. Granda, F. Rubiera, I. Suelves and R. Menéndez, *Fuel*, 2001, **80**, 1229–1238.
42 M. Siskin and A. R. Katritzky, *Chem. Rev.*, 2001, **101**, 825–836.
43 J. S. Francisco, *J. Chem. Phys.*, 1992, **96**, 1167–1175.
44 H. Kim, J. Ralph and T. Akiyama, *Bioenergy Res.*, 2008, **1**, 56–66.
45 N. Sathitsuksanoh, K. M. Holtman, D. J. Yelle, T. Morgan, V. Stavila, J. Pelton, H. Blanch, B. A. Simmons and A. George, *Green Chem.*, 2014, **16**, 1236–1247.
46 H. E. Gottlieb, V. Kotlyar and A. Nudelman, *J. Org. Chem.*, 1997, **62**, 7512–7515.
47 J. Rencoret, A. Gutierrez, L. Nieto, J. Jimenez-Barbero, C. B. Faulds, H. Kim, J. Ralph, A. T. Martinez and J. C. del Rio, *Plant Physiol.*, 2011, **155**, 667–682.
48 R. Kandiyoti, A. Herod, K. Bartle and T. Morgan, in *Solid Fuels and Heavy Hydrocarbon Liquids*, Elsevier, 2nd edn, 2017, pp. 343–436, DOI: 10.1016/B978-0-08-100784-6.00008-4.

